



POTSDAM-INSTITUT FÜR
KLIMAFOLGENFORSCHUNG

Originally published as:

Straiotto, B. G., [Marwan, N.](#), James, D. C., Seeley, P. J. (2023): Recurrence analysis discriminates martial art movement patterns. - European Physical Journal - Special Topics, 232, 1, 151-159.

DOI: <https://doi.org/10.1140/epjs/s11734-022-00684-6>

6 Recurrence analysis discriminates martial art movement patterns

7 B.G. Straiotto^{1, a}, N. Marwan², D.C. James¹ and P.J. Seeley¹

8 ¹ School of Applied Sciences, London South Bank University, London SE1 0AA, UK.

9 ² Potsdam Institute for Climate Impact Research, Member of the Leibniz Association, 14412 Potsdam, Germany.

10

11

12 **Abstract.** We aimed to determine whether combined application of principal components and recurrence
13 quantification analyses might serve to discriminate both spatial and temporal differences between backwards-
14 forwards movement patterns. Elite ($n = 9$) and nonelite ($n = 9$) martial artists were recorded using motion capture
15 techniques and features of whole-body movement defined at segment level were investigated by principal
16 components analysis. For both groups of subjects, four movement components explained $> 90\%$ of variability in the
17 data. Given our interest in temporal patterning, the time series derived from scores for each of the principal
18 components were subsequently subjected to recurrence quantification analysis, participant by participant. For the first
19 movement component, statistically significant differences between groups were detected for the recurrence measure
20 determinism ($p < 0.05$). For the third movement component, statistically significant differences were detected for the
21 recurrence measures laminarity and maxline ($p < 0.01$). Hence use of a combination of principal components and
22 recurrence techniques revealed quantitative differences between movements of the two subject groups, differences
23 that may represent more skilled motor control in the elite group related to the functional importance of these
24 apparently simple movement patterns.

25

26

27

28

29

30

31 ^a e-mail: brunostraiotto@gmail.com (corresponding author)
32

33	Abbreviations.	
34		
35	AP	Anterior-posterior
36	CoM	Centre of mass
37	%DET	% Determinism
38	DIS	Distributed
39	ENT	Entropy
40	%LAM	% Laminarity
41	MAXL	Maxline
42	ML	Medio-lateral
43	PCA	Principal components analysis
44	PM	Principal movement
45	RP	Recurrence plot
46	RQ(A)	Recurrence quantification (analysis)
47	SEM	Standard error in the mean
48	V	Vertical
49		

50 **1. Introduction**

51 Human movements are the consequence of many neural, muscular and skeletal components working together to
 52 achieve a desired outcome. Whilst a typical study may involve investigation of body kinematics, the aim
 53 ultimately is understanding of the mechanisms underpinning a movement and the neuromuscular strategies and
 54 synergies that serve to express the spatial and temporal features of intersegment coordination. The essence of
 55 some movements may be captured by use of simple kinematic techniques applied to, for example, a single limb;
 56 in other cases, investigation of the entire set of body segments is required.

57 Given our interest in whole-body coordination in the movements of martial artists, we adopted the
 58 approaches of previous researchers [1–3] for this study and applied principal components analysis (PCA) to
 59 centre of mass coordinates of the set of body segments. This method has conceptual and practical advantages: it
 60 reduces a high-dimensional dataset to a lower-dimensional set of independent components that is taken (on the
 61 basis of extent of variation) to represent the more important features of the data structure [4]. Whilst the starting
 62 data variables are normally highly correlated, the derived principal components are independent of each other.
 63 The contributions of the original variables to a given principal component are represented by their derived
 64 coefficients. In our case, these coefficients were related to the centre of mass body segment coordinates, and the
 65 set of coefficients indicated the forms and extents of collaboration amongst body segments over the entire time
 66 course of a particular principal movement.

67 It appeared quite unsatisfactory that the temporal dynamics of investigated movements had not been
 68 accounted for in deriving coefficient values, though time courses of the derived components were contained in
 69 the corresponding unidimensional scores [3]. We therefore investigated the temporal structures of these scores
 70 by plotting and quantification of recurrences [5].

71 The recurrence method is a nonlinear approach to analysis that involves unfolding time series data
72 within a multidimensional manifold [6]. It has provided insights into quite a variety of systems and situations
73 from variations in body posture to ecological and climate transitions to metal fracture [6-16]. The steps in
74 recurrence analysis are represented in Fig. 1 ((d) to (g)). Time-dependent signals that have been re-represented in
75 multidimensional space are characterized as the pattern of revisits of the movement trajectory to sub-regions of
76 that space. The revisits are known as *recurrences* and are a fundamental property of dynamical systems [5,17].
77 The fundamental equation for the recurrence matrix is provided below and described in detail in [5]:

$$78 \quad \mathbf{R}_{i,j} = \theta(\varepsilon - \|\vec{x}_i - \vec{x}_j\|), \quad i, j = 1, \dots, N, \quad (1)$$

79 where \mathbf{R} is the recurrence matrix, θ is the Heaviside function, ε is a predefined threshold distance, $\|\cdot\|$ is a
80 norm, \vec{x}_i and \vec{x}_j are the measured states (represented by m -dimensional state variables) of the system at times i
81 and j , and N is the number of observed states. Recurrence quantification analysis (RQA) produces a series of
82 measures quantifying the small-scale graphical patterns in a recurrence plot (RP), thereby allowing in-depth
83 description of (in our case) movement patterns, both generally and in relation to athletic performance (Fig. 1(f)
84 and (g)) [5,17]. The RQA measures are presented in the Methods section and reviewed in the Discussion.

85 Analysis of movement patterns of taekwondo players has been the subject of various studies aimed at
86 informing coaches on technique development and player performance in competition. Researchers have, for
87 example, investigated intra-limb coordination [18–20], patterns of kicking [21] and impact force characteristics
88 for the most common kicks [22,23]. We extended the investigation of taekwondo movement to the backwards-
89 forwards movements that are the basis for development of defensive and attacking actions by a player. We have
90 previously carried out simple kinematic analyses of backwards-forwards movements and have found no
91 differences between nonelite and elite groups of players. We therefore applied the alternative and more elaborate
92 analytical approach presented in this report (PCA followed by RQA) to investigate potential differences in these
93 movements for players of nonelite and elite status. The recurrence method was applied to determine differences
94 in the temporal organization of PCA data. In summary, we asked whether an alternative form of data analysis
95 might discriminate taekwondo movement patterns by skill level with the aims of assisting coaching practice and
96 relating taekwondo coordination to its underlying neuromuscular control. We postulated differences in
97 coordination patterns between elite and nonelite taekwondo players. Specifically, we hypothesised that RQA
98 measures of principal movements would reveal differences in the temporal structure of coordination between
99 players of different skill level.

100 [Insert Fig. 1 about here]

101 **2. Materials and methods**

102 **2.1 Participants and experimental protocol**

103 Eighteen elite and nonelite taekwondo players were recruited for this study (mean \pm standard error in the mean
104 (SEM); elite (8 males and 1 female; mean \pm SEM; age = 27.0 ± 0.4 y, mass = 74 ± 1 kg, height = 1.7 ± 0.1 m)
105 and nonelite (9 males; age = 35.0 ± 0.1 y, mass = 86 ± 3 kg, height = 1.8 ± 0.1 m). The elite taekwondo players
106 had competed at a minimum of A-class international and national levels for at least eight years. The nonelite
107 taekwondo players practised taekwondo at a recreational level and had a maximum of three years' experience.
108 The experimental protocol was given approval by London South Bank University Research Ethics Committee,
109 and all players provided written informed consent prior to taking part in the study.

110 The stance used during backwards-forwards movement is called *fixed stance*. The legs are split one and
111 a half shoulder widths apart, and the body is turned side-on to the opponent. The front foot is aligned with the
112 player-opponent axis while the back foot is twisted to be approximately perpendicular to that axis. The body
113 weight is shared evenly by the two legs (Fig. 1(a)). The players performed individualized warm-ups for 15
114 minutes. Following this, after a brief rest period, players performed the simplest of backwards-forwards
115 movements over a two-minute period from visual commands, mimicking a competition situation.

116

117 **2.2 Data collection and analysis**

118 In order to determine the movement kinematics of the taekwondo player during backwards-forwards
119 movements 12-mm diameter retroreflective markers were placed on the skin over anatomical landmarks (Table
120 A1, Appendix A) and the 3D coordinates of these markers were tracked using a motion capture system (Oqus 3-
121 Series, Qualisys AB, Gothenburg, Sweden). Each body segment (15 in total; Table B1, Appendix B) was
122 modelled in line with previously reported standards for tracking the upper [24] and lower [25] extremities, with
123 slight modification to suit this research [20]. Marker trajectories were collected at 300 Hz. The data analysis for
124 backwards-forwards movement had four main steps: (i) prescribing an articulated multi-segment system to
125 obtain centres of mass of each of the body segments (Fig. 1(a); Appendix B); (ii) principal components analysis
126 (PCA) on the centre of mass coordinates of these segments to identify the main movement patterns for
127 backwards-forwards movements (Fig. 1(b) and (c)); (iii) examination of temporal variability using recurrence
128 techniques (RPs and RQA) by analysing the time series formed by the principal component scores (Fig. 1(d) to
129 (g)); (iv) surrogate testing used to assess whether derived recurrence quantification measures were representative
130 of bona fide nonlinear dynamics in the principal component signals, or the product of random noise.

131 Prior to processing for PCA, the first and last 10 s of the centre of mass data were removed to eliminate
132 the influence of transient motions. The submitted data length was 30000 data points (100 s) for each player.
133 Segment masses were quantified as a 30000×45 matrix (frame [*rows*] \times centre of mass [*columns*]). Each row
134 of the matrix was interpreted as a 45-dimensional posture vector representing the centres of mass at a given point
135 in time. The 45-dimensions represent medio-lateral (ML), antero-posterior (AP) and vertical (V) directions for
136 each of the 15 segments. Representations were cut off after the first four principal components since the summed
137 eigenvalues reached a conventional standard of at least 90% of total variance [2] for both groups. MATLAB
138 software was used for PCA calculations (MATLAB 2013a and Statistics Toolbox 8.1, The MathWorks Inc,
139 Natick, MA, USA). The outputs from PCA are referred to as one-dimensional principal movements (PMs).

140

141 **2.3 Data processing for recurrence plotting and analysis**

142 The time series obtained by projecting the data onto the intrapersonal principal components were
143 subjected to recurrence plot and recurrence quantification analysis (Fig. 1(d) to (g)). As the name suggests, both
144 recurrence plotting and analysis seek understanding of the temporal structure of a time series in terms of
145 recurring patterns in the data. The data are not, however, examined in their original dimension, rather they are
146 “unfolded” into multiple dimensions. The first step in the process is the selection of a time scale for the analysis
147 (τ), the second step is derivation of the number of dimensions to be employed (m) and the final step is the setting
148 of a distance criterion (ϵ , in m dimensions) for the revisiting (i.e. recurrence) of a region of phase space along the
149 time-dependent data trajectory. The procedures have been described in detail in [5,17].

150 A time delay of $\tau = 7$ was taken as the time of the first local minimum of the mutual average
151 information function for the time series [26]. The value for the embedding dimension for recurrence analysis was
152 set to 5 according to the false nearest neighbours method [17]. A threshold (ϵ) value of 10% of the maximum
153 phase space diameter and the Euclidean norm were employed, these being consistent with previous researches
154 using recurrence analysis to evaluate human movement [6,27–29].

155 A windowing technique was used to verify consistency of parameter estimation and to detect any
156 changes and transitions in the time series [30]. The data were sectioned in large windows (10000 points), each
157 33 s long. Adjacent windows were offset by 5000 points yielding a 50% overlap. Five windows were used for
158 recurrence plot and RQA calculations, which employed the Cross Recurrence Plot Toolbox for MATLAB [31].

159 RQA produces a series of measures of complexity that both quantify the small-scale graphical patterns
160 in an RP (Fig. 1(f) and (g)) [5,17] and provide insight into dynamical features of a time series. The measures

161 used in this study were as follows. (i) Determinism (%DET) is a measure of the predictability of a data series:
162 higher percentage values indicating higher predictability. (ii) Entropy (ENT) is one quantification of the degree
163 of regular/irregular patterning (the orderliness) in a data series, i.e. higher ENT values are associated with less
164 regular patterns (at least when considering non-periodic signals, see [32]). (iii) Laminarity (%LAM) gives a
165 measure of states of low variation and persistence (pauses, breaks) in a time series, i.e. %LAM increases with the
166 incidence of states of low variation or high persistence. (iv) Maxline (MAXL) gives a measure of the stability of
167 a system, higher values meaning higher stability or longer persistence.

168 The variation of these measures were tested for statistical significance by a surrogate test: (i) Fourier
169 transformation of the signal; (ii) randomization of the transformed phase values (while amplitude values
170 remained constant); and (iii) inverse Fourier transformation [33]. The null hypothesis for this statistical test
171 assumes that the time series was the result of a linear Gaussian stochastic process. The hypothesis test was
172 carried out by computing 150 surrogates on the PM score followed by calculation of %DET, MAXL, ENT and
173 %LAM values for each of the surrogate time series. These were then compared statistically to their original
174 counterparts. The null hypothesis was rejected at a level of significance of $\alpha = 0.01$ as proposed by Myers [34].
175 The RQA measures derived from the original data were significantly different ($p < 0.01$) from those of the
176 surrogates (Fig. 2), which supports the validity of reporting them as nonlinear measures of the principal
177 movement time series.

178 [Insert Fig. 2 about here]

179 **2.4 Statistical analysis**

180 SPSS software (version 21; SPSS Inc, Chicago, IL, USA) was used for calculation of all statistics. The
181 eigenvalues for the first four principal movements (PMs) were normally distributed for both elite and nonelite
182 groups as assessed by Kolmogorov-Smirnov tests (all $p > 0.05$) and there was homogeneity of variance as
183 evaluated by Levene's test (all $p > 0.05$). Independent t -tests were therefore used to determine the significance of
184 differences between elite and nonelite players. Kolmogorov-Smirnov tests showed that the RQA measurements
185 did not fit normality of distribution ($p < 0.05$). Therefore, data values were square root transformed and
186 independent t -tests were then carried out to determine the significance of differences between elite and nonelite
187 athletes. The windowing technique served to indicate that RQA measurement values were approximately
188 constant over the trial period (i.e., there was no evidence of player fatigue) so the average of all windows ($n = 5$)
189 for each RQA measurement was used in testing for differences between elite and nonelite groups. The
190 significance level was set at $\alpha = 0.05$.

191

192 **3. Results**

193 Table 1 reports the eigenvalues (mean \pm SEM) for the backwards-forwards movement task. The contribution of
194 the first component to overall variability was less for elite players as compared with nonelite ($37 \pm 1\%$ versus 46
195 $\pm 4\%$ respectively) with greater elite contributions to the second to fourth components. The only significant
196 difference between elite and nonelite athletes was found for the third component ($19 \pm 2\%$ versus $16 \pm 2\%$; $p <$
197 0.01).

198 [Insert Table 1 about here]

199 The eigenvector coefficients shown in Fig. 3 are arranged by group and provide information about the
200 extent to which individual coordinates for body segment masses contribute to the principal movements.
201 Qualitatively, and in contrast to eigenvalue results, there are notable differences between coefficient values for
202 elite and nonelite players. Data are presented for antero-posterior (AP), medio-lateral (ML) and vertical (V) axes
203 of segment displacement. In order to represent something of the character of each of the principal movements we
204 have named them after elite patterns as: PM1AP-V, PM2ML, PM3AP+V and PM4DIS (distributed), "-" and "+"
205 indicating the relative signs of AP and V coordinate contributions. For PM1AP-V coefficients, movement along
206 the AP axis is the main contributor for elite taekwondo performance. In contrast, nonelite backwards-forwards
207 movement performance is characterized less for the AP axis in favour of greater vertical movement. While ML
208 coefficients are differentiated across body segments for elite players, the corresponding components for nonelite
209 are hardly differentiated. The PM2ML coefficient profiles for elite and nonelite taekwondo players are quite
210 similar, with the predominant movement occurring along the ML axis.

211 For PM3AP+V coefficients, both groups of players make use of movement in all three directions and
212 magnitudes are roughly comparable, though less so for V in the elite group. However, nonelite demonstrate
213 greater differentiation in movement in all three directions across body segments, particularly in the vertical
214 direction. Notable differences in PM4DIS coefficients are comparatively greater utilisation of ML movement in
215 the pelvis and thigh for the elite group (Fig. 3). Overall, the eigenvector coefficients serve to distinguish in detail
216 between patterns of elite and nonelite movement at segment level. (Given the principal focus on recurrence
217 analysis of movements for this paper, a detailed analysis of eigenvector coefficients is not presented. Since the
218 group sizes were comparatively small and some players executed backwards-forwards movements in a markedly
219 idiosyncratic manner a full account of coefficients would take this paper beyond its space allocation.)

220

[Insert Fig. 3 about here]

221 Examples of backwards-forwards movement recurrence plots for each of the four PMs from an elite and
222 nonelite player are illustrated in Fig. 4. Between players and PMs, a variety of recurrence plot typologies were
223 demonstrated. These included homogenous, single isolated, drift and disrupted patterns [5]. For each recurrence
224 plot, four RQA measures (%DET, ENT, %LAM and MAXL) were derived (Fig. 5).

225 [Insert Fig. 4 about here]

226 For %DET (percent determinism, Fig. 5(a)), a significant difference between groups was found for
227 PM1AP-V ($p < 0.05$). Here, the nonelite athletes demonstrated greater predictability in operating backwards-
228 forwards movements ($98.4 \pm 1.0\%$ vs $97.5 \pm 1.0\%$). For ENT (entropy, Fig. 5(b)), there were no significant
229 differences between groups across the four PMs. A significant difference between groups was found for %LAM
230 (percent laminarity, Fig. 5(c)) for PM3AP+V ($p < 0.01$). Here, the elite athletes demonstrated greater %LAM in
231 their backwards-forwards movements ($69 \pm 8\%$ vs $40 \pm 10\%$). Finally, a significant group difference was found
232 for MAXL (maxline, Fig. 5(d)) for PM3AP+V ($p < 0.01$) with elite athletes demonstrating greater stability of
233 backwards-forwards movement (1600 ± 300 points vs 430 ± 320 points).

234 [Insert Fig. 5 about here]

235 **4. Discussion**

236 We sought and identified group-wide differences in the spatial and temporal structures of backwards-forwards
237 movements of our taekwondo martial artists.

238 The PCA approach has various benefits in that the entire movement is described without use of pre-
239 selected variables [1,3], rather movement is summarised as a limited set of sub-movements, and the analysis has
240 the capacity to access hidden variables inherent to the movement pattern. The set of PM coefficients provided
241 valuable information about the degree to which individual segment centre of mass coordinates contributed to
242 corresponding component movements and to contrasts between elite and nonelite player groups. The
243 eigenvalues, however, provided only limited insight into movement patterns and inter-group comparisons. To
244 make appropriate use of PCA, it appears important to examine the eigenvector coefficients in order to understand
245 – contextually – the characteristics of each principal movement. This study has taken a somewhat different
246 approach to the application of PCA since previous work has relied more heavily on eigenvalues and scores for
247 interpretation [4,35,36].

248 Whilst PCA produces time series for movement components (the scores), it does not access the
249 temporal structure of the components. For this purpose, we employed recurrence plots and recurrence
250 quantification analysis to identify facets of the movement components that describe predictability, uncertainty,

251 states of stability and low variation. We were, thus, able to gain insight into the movement patterns in some
252 depth and identify ways in which the elite and nonelite groups differed in their execution of backwards-forwards
253 movements. A primary concern in relation to RQA relates to the source of data variation. That is, is the variation
254 in a time series deterministic or is it the result of random noise? To this end we used the Fourier transform
255 surrogates to establish the existence of nonlinear dynamics underlying our experimental data (Fig. 2). We
256 confirmed nonlinearity in our data set, leading us to conclude that the observed player responses do in fact reflect
257 variation in movement due to neuromuscular control.

258 Movements of the elite group for PM1 anterior-posterior and vertical axes were highly predictable
259 (%DET of 97.5%), though less predictable than those of the nonelite group, and also more stable (higher
260 MAXL), representing an alternative dynamics pattern (higher %LAM) also for PM3 anterior-posterior and
261 vertical axes. This behaviour is reflected in eigenvector coefficients for PM3 anterior-posterior and vertical
262 directions (Fig. 3). For the elite taekwondo players anterior-posterior and vertical movements contributed
263 strongly to PM3 anterior-posterior and +vertical, for medio-lateral less so. The distribution of coefficient values
264 across body segments was also more uniform. In contrast, nonelite players' coefficient contributions to anterior-
265 posterior and vertical PM3 were similar for medio-lateral, anterior-posterior and vertical axes, though there was
266 greater coefficient variation across the body than for elites, and values for right and left limbs were not
267 equivalent. This relates to a lower MAXL value and greater variation in time (lower %LAM) for PM3 anterior-
268 posterior and vertical axes for nonelite taekwondo players.

269 The PM3 anterior-posterior and vertical results in particular suggest that elite and nonelite players use
270 different approaches to manage the task variables. This can be related to the controlled/uncontrolled manifold
271 perspective [37]. In this view [37], variables that do not influence task outcome (the uncontrolled manifold) are
272 allowed to fluctuate. For example, in relation to work on shooting, movement of the gun barrel along its axis is
273 not subject to control but movement perpendicular to its axis, having a direct influence on shot outcome, is
274 tightly controlled [38]. Backwards-forwards movements are used by a taekwondo player to gauge distance to an
275 opponent and to mount and escape attacks. A nonelite player may use backwards-forwards movements in a more
276 passive way and be less inclined to arrange their movements as a springboard for attack or for active defence that
277 will involve an immediate counterattack, i.e. their backwards-forwards movements may be tuned less to
278 function. The analysis through combined use of PCA and recurrence analysis allows insights into the relative
279 importance of controlling or failing to control particular movement variables.

280 Whilst statistically significant differences by group were obtained in relation to some RQA measures
281 and principal movements, other data trends are worthy of note. For %DET (Fig. 5(a)), there was a trend of
282 decreased predictability for anterior-posterior and vertical for the movement series PM1 to PM4 (distributed).
283 Entropy values decreased along this series also (Fig. 5(b)). Fluidity of movement, as registered by %LAM, was
284 fairly consistent over principal movements, except for medio-lateral PM2 for which increased transitioning was
285 apparent in the movements of both groups (Fig. 5(c)). Finally, the stability of movement (MAXL, Fig. 5(d))
286 remained consistent across the series of principal movements, except for medio-lateral PM2 where instability
287 was apparent in the movement of both groups. Across the set of RQA measurements, medio-lateral PM2 is
288 distinctive.

289 Limitations to our study and report are acknowledged. Whilst a body of data was collected under
290 carefully controlled conditions, experimentation was modest in scope in that each of the groups had only nine
291 participants. Comparisons therefore had limited statistical power. Assignment to groups was based somewhat
292 arbitrarily on taekwondo experience: some “nonelite” individuals may have executed backwards-forwards
293 movements in an elite manner despite their more limited experience. In addition, comparatively large variation
294 between the movement patterns of players was evident both from differences in RP patterns (Fig. 4) and from
295 comparatively large SEM values (Fig. 5), and this naturally made statistical significance more difficult to
296 achieve.

297 We report, according to conventional standards, the discrimination of movement patterns between our
298 elite and nonelite groups. There is group-level generality but also player individuality in the movements
299 recorded. In some cases, elite variation was greater than nonelite and in some cases it was less. One can therefore
300 put forward alternative views, namely that large elite variation was functional and derived from experience and
301 that large nonelite variation was a result of lack of control and lack of experience. Variation in backwards-
302 forwards movements within subject groups may simply be a representation of the individuality of solution to a
303 movement “problem”, functional or not. Nevertheless, statistically significant group-level differences were
304 noted. A straightforward interpretation is that elite players have refined these relatively simple movements
305 through extended training and competition experience. PCA, through the sets of coefficient values, revealed
306 qualitative differences between elite and nonelite backwards-forwards movements. The combination of PCA and
307 RQA revealed quantitative differences in temporal variation in the principal movements. Given the availability
308 of motion capture, coordination assessments of individual athletes may be carried out and these methods may be
309 of assistance to coaches in analysing movements of their athletes.

310 **Acknowledgments.**

311 The authors are grateful to Kiros Karamanidis and Matthias König for their review of the manuscript.

312 **References**

- 313 1. P. Federolf, K. Tecante, and B. Nigg, *J Biomech* **45**, 1127 (2012).
- 314 2. A. Daffertshofer, C. J. C. Lamoth, O. G. Meijer, and P. J. Beek, *Clin Biomech* **19**, 415 (2004).
- 315 3. V. C. Ramenzoni, M. A. Riley, K. Shockley, and A. A. Baker, *Hum Mov Sci* **31**, 1253 (2012).
- 316 4. N. F. Troje, *J Vis* **2**, 371 (2002).
- 317 5. N. Marwan, M. Carmen Romano, M. Thiel, and J. Kurths, *Phys Rep* **438**, 237 (2007).
- 318 6. M. A. Riley, R. Balasubramaniam, and M. T. Turvey, *Gait Posture* **9**, 65 (1999).
- 319 7. J. F. Donges, R. V. Donner, M. H. Trauth, N. Marwan, H.-J. Schellnhuber, and J. Kurths, *Proc Natl Acad Sci*
- 320 **108**, 20422 (2011).
- 321 8. T. Westerhold, N. Marwan, A. J. Drury, D. Liebrand, C. Agnini, E. Anagnostou, J. S. K. Barnet, S. M.
- 322 Bohaty, D. De Vleeschouwer, F. Florindo, T. Frederichs, D. A. Hodell, A. E. Holbourn, D. Kroon, V. Lauretano,
- 323 K. Littler, L. J. Lourens, M. Lyle, H. Pälke, U. Röhl, J. Tian, R. H. Wilkens, P. A. Wilson, and J. C. Zachos,
- 324 *Science (80-)* **369**, 1383 (2020).
- 325 9. V. L. Hilarov, *Phys Solid State* **59**, 1789 (2017).
- 326 10. G. Zurlini, N. Marwan, T. Semeraro, K. B. Jones, R. Aretano, M. R. Pasimeni, D. Valente, C. Mulder, and I.
- 327 Petrosillo, *Landsc Ecol* **33**, 1617 (2018).
- 328 11. J. M. Haddad, R. E. a Van Emmerik, J. S. Wheat, and J. Hamill, *Exp Brain Res* **190**, 431 (2008).
- 329 12. S. Ikegawa, M. Shinohara, T. Fukunaga, J. P. Zbilut, and C. L. Webber, *Biol Cybern* **82**, 373 (2000).
- 330 13. K. Shockley and M. A. Riley, in *Recurrence Quantif Anal*, edited by C. L. J. Webber and N. Marwan
- 331 (Springer, New York, 2015), pp. 399–421.
- 332 14. C. L. J. Webber, M. A. Schmidt, and J. M. Walsh, *J Appl Physiol* **78**, 814 (1995).
- 333 15. A. M. Nkomidio, E. K. Ngamga, B. R. N. Nbandjo, J. Kurths, and N. Marwan, *Entropy* **24**, (2022).
- 334 16. T. Semeraro, A. Luvisi, A. O. Lillo, R. Aretano, R. Buccolieri, and N. Marwan, *Remote Sens* **12**, 907 (2020).
- 335 17. C. L. J. Webber and J. P. Zbilut, in *Tutorials Contemp Nonlinear Methods Behav Sci*, edited by M. A. Riley
- 336 and G. C. Van Orden (Retrieved March 1, 2005, from www.nsf.gov/sbe/bcs/pac/nmbs/nmbs.jsp, 2005), pp. 26–
- 337 94.
- 338 18. F. Quinzi, V. Camomilla, F. Felici, A. Di Mario, and P. Sbriccoli, *J Electromyogr Kinesiol* **23**, 140 (2013).
- 339 19. I. Estevan, J. Freedman Silvernail, D. Jandacka, and C. Falco, *J Sports Sci* **34**, 1766 (2016).
- 340 20. B. G. Straiotto, D. P. Cook, D. C. James, and P. J. Seeley, *J Appl Biomech* **37**, 513 (2021).

- 341 21. I. Estevan and C. Falco, *Biol Sport* **30**, 275 (2013).
- 342 22. G. Fife, W. Pieter, D. O'Sullivan, D. Cook, and T. Kaminski, *Br J Sport Med* **45**, 318 (2011).
- 343 23. D. O'Sullivan, C. Chung, K. Lee, E. Kim, S. Kang, T. Kim, and I. Shin, *J Sport Sci Med* **8**, 10 (2009).
- 344 24. G. Wu, F. C. T. van der Helm, H. E. J. Veeger, M. Makhssous, P. Van Roy, C. Anglin, J. Nagels, A. R.
- 345 Karduna, K. McQuade, X. Wang, F. W. Werner, and B. Buchholz, *J Biomech* **38**, 981 (2005).
- 346 25. T. D. Collins, S. N. Ghousayni, D. J. Ewins, and J. A. Kent, *Gait Posture* **30**, 173 (2009).
- 347 26. S. A. Myers, J. M. Johanning, I. I. Pipinos, K. K. Schmid, and N. Stergiou, *Ann Biomed Eng* **41**, 1692
- 348 (2013).
- 349 27. C. A. Coey, M. Washburn, and J. M. Richardson, in *Transl Recurrence*, edited by N. Marwan, M. Riley, A.
- 350 Giuliani, and C. L. J. Webber (Springer, New York (USA), 2014), pp. 173–186.
- 351 28. F. S. Labini, A. Meli, Y. P. Ivanenko, and D. Tufarelli, *Gait Posture* **35**, 48 (2012).
- 352 29. K. Shockley, in *Tutorials Contemp Nonlinear Methods Behav Sci*, edited by M. A. Riley and G. C. Van
- 353 Orden (Retrieved March 1, 2005, from www.nsf.gov/sbe/bcs/pac/nmbs/nmbs.jsp, 2005), pp. 142–177.
- 354 30. C. L. J. Webber and N. Marwan, in *Recurrence Quantif Anal*, edited by N. Marwan and C. L. J. Webber,
- 355 (Springer, New Jersey, 2015), pp. 3–43.
- 356 31. N. Marwan, Cross Recurrence Plot Toolbox, available online at tocsy.pik-potsdam.de/CRPtoolbox (2013).
- 357 32. K. H. Kraemer and N. Marwan, *Phys Lett Sect A Gen At Solid State Phys* **383**, (2019).
- 358 33. S. A. Myers, in *Nonlinear Anal Hum Mov Var*, edited by N. Stergiou (CRC Press, Taylor & Francis Group,
- 359 New York, 2016), pp. 29–53.
- 360 34. S. A. Myers, in *Var Nonlinear Anal Hum Mov*, edited by N. Stergiou (CRC Press, Taylor & Francis Group,
- 361 New York, 2016), pp. 111–171.
- 362 35. P. Federolf, K. Boyer, and T. P. Andriacchi, *J Biomech* **46**, 2173 (2013).
- 363 36. J. Verrel, M. Lövdén, M. Schellenbach, S. Schaefer, and U. Lindenberger, *Psychol Aging* **24**, 75 (2009).
- 364 37. J. P. Scholz and G. Schöner, *Exp Brain Res* **126**, 289 (1999).
- 365 38. J. P. Scholz, G. Schöner, and M. L. Latash, *Exp Brain Res* **135**, 382 (2000).

366

367

368 **Figure Captions**

369 **Fig. 1** Graphical presentation of the methods applied to backwards-forwards movement data, illustrated for a
370 single player. (a) Backwards-forwards movement centre of mass displacements obtained from an articulated
371 multi-segment system. (b) Calculation of PCA on the centre of mass displacements of 15 rigid segments. (c) A
372 principal movement (PM) describing the behaviour of the whole body (PM2ML). (d) State space reconstruction
373 in 3D of the structure of a dynamical system for a single PM. (e) Calculation of the radius of the neighbourhood
374 in which recurrent states occur. (f) Recurrence plot of one of the PMs. (g) RQA measures used in this study:
375 determinism (%DET), entropy (ENT), laminarity (%LAM) and maxline (MAXL).

376 **Fig. 2** Outcomes of surrogation analysis for a single PM and a single player. The open circles are surrogate
377 values of %DET (a), MAXL (b), ENT (c) and %LAM (d). The solid circles represents the original data. The
378 solid black lines indicate the 99% significance border of the rank order statistics. The RQA measurements for the
379 original data were significantly different from those of the surrogates ($p < 0.01$).

380 **Fig. 3** Eigenvector coefficients from PCA for body segment masses for the backwards-forwards movement task.
381 Lightly shaded, open and darkly shaded bars represent ML, AP and V movements respectively. Columns
382 represent average values over the player group; error bars are corresponding \pm SEMs. The masses are reported in
383 order from head to foot.

384 **Fig. 4** Recurrence plots from representative elite and nonelite players for the first four PMs for the backwards-
385 forwards movement task. Norm = Euclid; Delay = 7; Embedding dimension = 5; Threshold = 0.1.

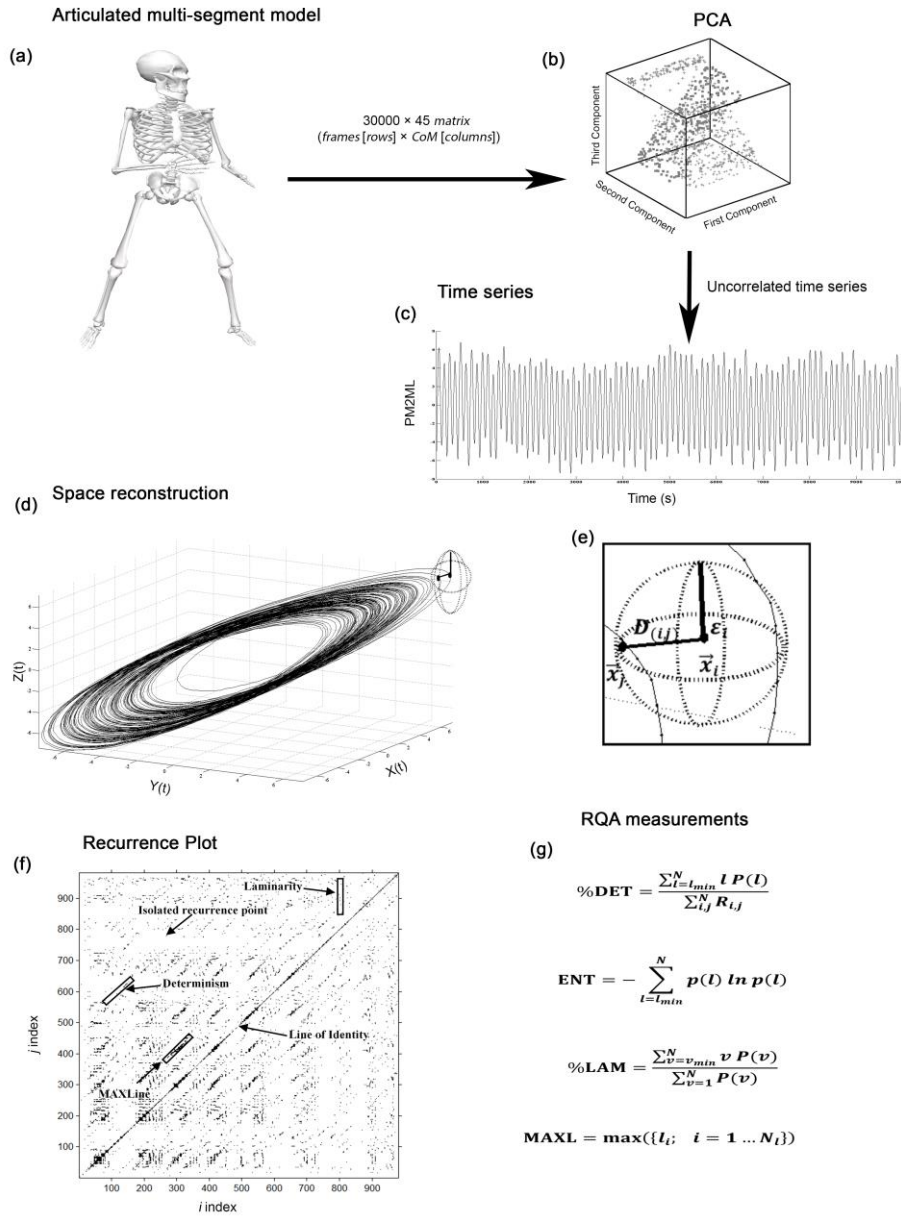
386 **Fig. 5** Results of RQA measurement for the first four PMs for the backwards-forwards movement task for elite
387 (filled square) and nonelite (open square) taekwondo players. (a) %DET, (b) ENT, (c) %LAM and (d) MAXL
388 for PM scores averaged with over the five data windows (\pm SEM). * indicates a significant difference between
389 elite and nonelite values on square-root-transformed data.

390

391 **Table Captions**

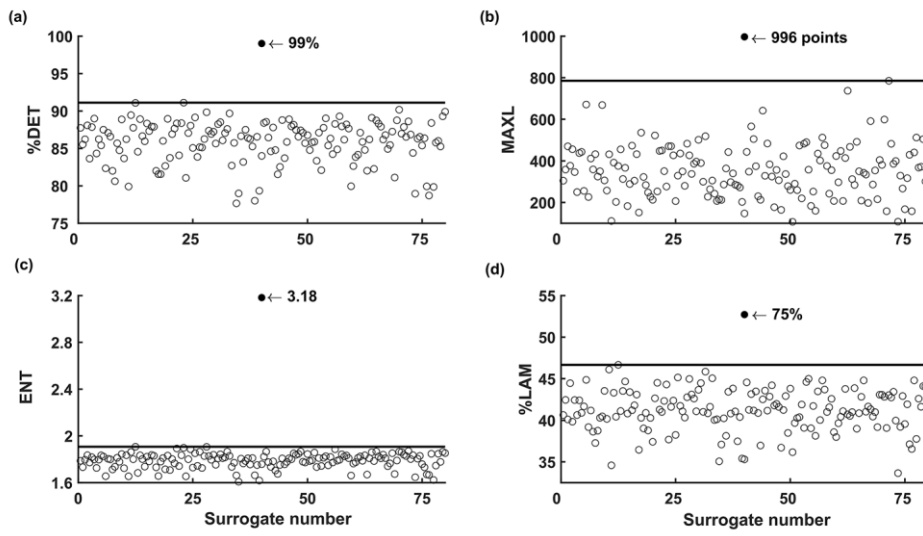
392 **Table 1** Eigenvalues of the first four principal movements for backwards-forwards movements for elite and
393 nonelite taekwondo players.

394



396

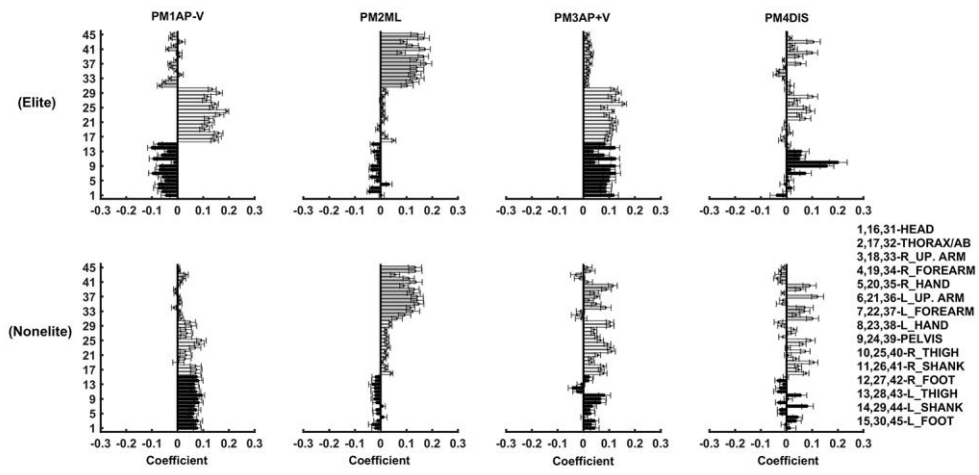
397



399

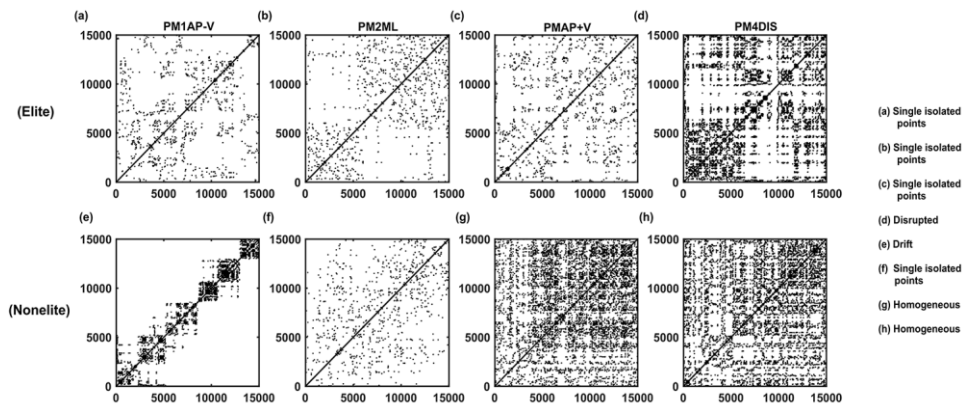
400

401 Fig. 3



402

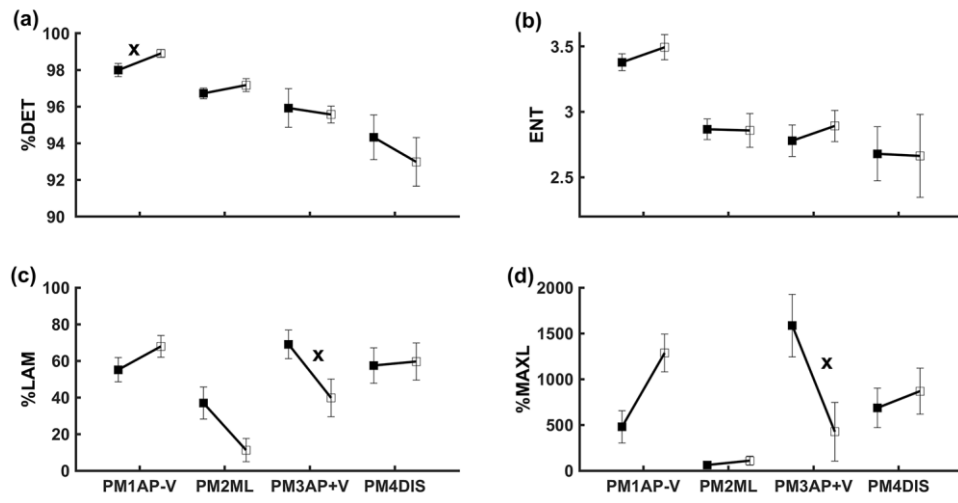
403



405

406

407 Fig. 5



408

409

410 **Table 1**

	First (PM1AP-V)	Second (PM2ML)	Third (PM3AP+V)	Fourth (PM4DIS)
Elite	37 (± 1)* %	27 (± 1)%	19 (± 2)%	7 (± 1)%
Nonelite	46 (± 4)%	25 (± 1)%	16 (± 2)%	6 (± 1)%
$p^{\#}$	0.087	0.91	0.0040	0.36

411

412

413 Eur. Phys. J. Special Topics (2022)
414 © EDP Sciences, Springer-Verlag 2022
415 DOI : 10.1140/xxxxx (will be inserted by the publisher)
416

417 **Appendix**

418 **Recurrence analysis discriminates martial art movement patterns**

419 B.G. Straiotto^{1,a}, N. Marwan², D.C. James¹ and P.J. Seeley¹

420 ¹ School of Applied Sciences, London South Bank University, London SE1 0AA, UK.

421 ² Potsdam Institute for Climate Impact Research, Member of the Leibniz Association, 14412 Potsdam, Germany.

422 .

423

424

425

426

427

428

429

430

431

432

433

434

435

436

437

438

439

440

441

442 ^a e-mail: brunostraiotto@gmail.com (corresponding author)
443

444 **APPENDIX A.**

445 Marker definition

446 **Table A1** Marker definition and tracking set up.

Segment	Labels	Numbers	Definition	Tracking	Description
Head	TMJ	2	✓	✓	Temporomandibular Joint
	BHD	2	✓	✓	Back Head
Thorax	IC	2	✓	✓	Iliac Crest
	AC	2	✓	✓	Acromion
	C7	1	✓	✓	Seventh Cervical Vertebra
	SSN	1	✓	✓	Suprasternal Notch
	XIPH	1	✓	✓	Xiphoid Process
	T10	1	✓	✓	Tenth Thoracic Vertebra
	CP	2	✓		Coracoid Process
	AA	2	✓		Angulus Acromialis
	AI	2	✓	✓	Angulus Inferior
TS	2	✓	✓	Trigonum Spinae Scapulae	
Upper arm	LHEC	2	✓		Lateral Epicondyle of the Humerus
	MHEC	2	✓		Medial Epicondyle of the Humerus
	UA1	2		✓	Upper arm 1
	UA2	2		✓	Upper arm 2
	UA3	2		✓	Upper arm 3
Forearm	RSP	2	✓	✓	Radial Styloid Process
	USP	2	✓	✓	Ulnar Styloid Process
	FA1	2		✓	Forearm 1
	FA2	2		✓	Forearm 2
	FA3	2		✓	Forearm 3
Hand	CARP3	2	✓	✓	Third Metacarpophalangeal Joint
Pelvis	ASIS	2	✓	✓	Anterior Superior Iliac Spine
	PSIS	2	✓	✓	Posterior Superior Iliac Spine
Thigh	LEC	2	✓		Lateral Epicondyle of the Femur
	MEC	2	✓		Medial Epicondyle of the Femur
	THI1	2		✓	Thigh 1
	THI2	2		✓	Thigh 2
	THI3	2		✓	Thigh 4
Shank	THI4	2		✓	Thigh 4
	LMAL	2	✓		Lateral Malleolus
	MMAL	2	✓		Medial Malleolus
	SHK1	2		✓	Shank 1
	SHK2	2		✓	Shank 2
Foot	SHK3	2		✓	Shank 3
	SHK4	2		✓	Shank 4
	MET1D	2	✓		First Metatarsal
	MET5D	2	✓		Fifth Metatarsal
	CAL	2	✓		Calcaneus
Foot	FOT1	2		✓	Foot 1
	FOT2	2		✓	Foot 2
	FOT3	2		✓	Foot 3
Individual marker		48	46	26	
Cluster marker		34		34	
Total		82	46	60	

447

448










449 **APPENDIX B.**

450 Multi-segment model

451 Each player was represented as an articulated multi-segment system with 15 rigid segments (head, thorax, upper
452 arms, forearms, hands, pelvis, thighs, shanks and feet; see anatomical coordinate system below). The inverse
453 kinematics technique was applied to the model with specific joint constraints (Table A2). Upper extremity and
454 lower extremity inverse kinematic linkages were created, which started at the pelvis segment for the lower
455 extremity, and at the thorax segment for the upper extremity. For each joint, a set of constraints was enforced,
456 where segments could rotate with three degrees of freedom, but not translate with respect to the adjacent
457 segment. The centre of masses of the segments were measured from the global coordinate system. Visual3D
458 software (C-Motion Inc, Germantown, MD, USA) was used to build the articulated multi-segment system and
459 for centre of mass calculations.

460

Table B1 Anatomical coordinate system and inverse kinematics for each body segment.

Segments	Coordinate systems x , y and z	IK constraint	IK unconstraint
	Origin: Midpoint between R_AC and L_AC x : Oriented from L_AC to R_TMJ pointing right y : Perpendicular to x in the plane defined by L_AC to R_AC and midpoint between R_BHD and L_BHD z : Perpendicular to both x and y pointing upwards	Translation x, y, z	Rotation x, y, z
	Origin: Waist joint - midpoint between R_IC and L_IC x : Oriented from L_IC to R_IC pointing right y : Perpendicular to x in the plane defined by R_IC, L_IC and midpoint between R_AC and L_AC z : Perpendicular to both x and y pointing upwards		Rotation x, y, z Translation x, y, z
	Origin: Shoulder joint centre (SJC) z : Oriented from elbow joint centre (EJC) to shoulder joint centre (SJC) pointing upwards x : Perpendicular to z in the plane defined by LHEC, MHEC and SJC pointing right y : Perpendicular to both x and z pointing forwards	Translation x, y, z	Rotation x, y, z
	Origin: EJC - midpoint between LHEC and MHEC z : Oriented from midpoint between RSP and USP to EJC pointing upwards x : Perpendicular to z in the plane defined by RSP, USP and EJC pointing right y : Perpendicular to both x and z pointing forwards	Translation x, y, z	Rotation x, y, z
	Origin: CARP3 z : Oriented from CARP3 to midpoint between RSP and USP pointing upwards x : Perpendicular to z in the plane defined by CARP3 and midpoint between RSP and USP pointing right y : Perpendicular to both x and z pointing forwards	Translation x, y, z	Rotation x, y, z
	Origin: Midpoint between R_ASIS and L_ASIS x : Oriented from L_ASIS to R_ASIS pointing right y : Perpendicular to x in the plane defined by R_ASIS, L_ASIS and the midpoint between R_P SIS and L_P SIS. z : Perpendicular to both x and y pointing upwards		Rotation x, y, z Translation x, y, z
	Origin: Hip joint centre (HJC) z : Oriented from midpoint between LEC and MEC (KJC) to HJC pointing upwards x : Perpendicular to z in the plane defined by LEC, MEC and HJC pointing right y : Perpendicular to both x and z pointing forwards	Translation x, y, z	Rotation x, y, z
	Origin: Knee joint (midpoint between LEC and MEC) z : Oriented from midpoint between LMAL and MMAL to KJC pointing upwards x : Perpendicular to z in the plane defined by LMAL, MMAL and KJC pointing right y : Perpendicular to both x and z pointing forward	Translation x, y, z	Rotation x, y, z
	Origin: Ankle joint (midpoint between LMAL and MMAL) z : Oriented from midpoint between LMAL and MMAL to midpoint between MET1D and MET5D pointing upwards x : Perpendicular to z in the plane defined by LMAL, MMAL, MET1D and MET5D pointing right y : Perpendicular to both x and z pointing forward	Translation x, y, z	Rotation x, y, z